doi:10.3788/gzxb20184709.0916005

磁控溅射结合脉冲激光制备钛掺杂硅薄膜的研究

王凯,李晓红,张延彬,温才,刘德雄
(西南科技大学 理学院 极端条件物质特性联合实验室,四川 绵阳 621000)

摘 要:发展了一种改进的新型超掺杂工艺,通过真空磁控溅射多层镀膜后结合 532 nm 波长可见纳秒脉冲激光熔融处理,进行超掺杂钛的硅薄膜材料的制备,并对材料的超掺杂层的性质和红外吸收性能进行了探究.结果表明,硅膜层中掺杂的钛原子的百分比浓度超过 1%左右,对应钛原子浓度约为 5×10^{20} cm^{-3}左右,超过钛在硅中形成超掺杂所对应的原子浓度.钛超掺杂层的厚度超过 200 nm 左右,相对传统工艺具有明显提升,并且钛原子的浓度变化范围不超过 20%,分布比较均匀.小角度 X 射线衍射测试表明经过可见脉冲激光熔融处理后的硅薄膜层材料结晶度为 25%左右,呈多晶结构.同时红外吸收谱测试表明,样品的钛掺杂硅膜层在大于 1 100 nm 波长的区域具有很高的红外吸收效果,最高的红外吸收系数达到 1.2×10^{4} cm^{-1},远超过单晶硅材料.具有比较明显的亚能带吸收的特征,呈现出 E_c-0.26 eV 的掺杂能级.霍尔效应测试表明硅膜层具有较高的载流子浓度,超过了 8×10^{18} cm^{-3}.

关键词:激光物理;脉冲激光;磁控溅射;硅;超掺杂;深能级杂质
中图分类号:O472+.3 **文献标识码**:A **文章编号**:1004-4213(2018)09-0916005-8

Study of Titanium-doped Silicon Films Prepared by Magnetron Sputtering and Nanosecond Pulsed Laser

WANG Kai, LI Xiao-hong, ZHANG Yan-bing, WEN Cai, LIU De-xiong
(*Joint Laboratory for Extreme Conditions Matter Properties, School of Science, Southwest University of Science and Technology, Mianyang, Sichuan*, 621000, *China*)

Abstract: An improved hyper-doping process has been developed which combines the vacuum magnetron sputtering coating and the 532 nm wavelength visible nanosecond pulse laser melting to prepare the silicon thin films of titanium doping. The characteristics of hyper-doped layer and the infrared light absorption properties of silicon thin film were studied. The X-ray photoelectron spectroscopy shows that the titanium concentration of doping layer of sample is more than 1% (the corresponding titanium atom concentration is about 5×10^{20} cm^{-3}), higher than the hyper-doping concentration of titanium in silicon. And the thickness of hyper-doping layer is more than 200 nm which improves obviously compared with traditional technology. The variable range of the concentration of titanium atoms is not more than 20%, and the atom distribution is more homogeneous. The glancing incidence X-ray diffraction pattern shows that the crystallinity of the silicon thin film layer is polycrystalline structure and about 25% around after pulsed laser melting. At the same time, the infrared light absorption measurement shows that the hyper-doping silicon thin film has high infrared absorptivity in wavelength larger than 1 100 nm. The highest infrared light absorption coefficient of sample is almost to 1.2×10^{4} cm^{-1}, which is far more than that of monocrystalline silicon. The material has obvious characteristics of sub-band absorption and shows a

Foundation item: The National Natural Science Foundation of China (No.11204250), the Scientific Research Fund of Sichuan Provincial Education Department (No.17CZ0038) and the Office of Science & Technology and Intellectual Property of Mianyang (No.16G-01-11), Postgraduate Innovation Fund Project by Southwest University of Science and Technology (No.17ycx071).
First author: WANG Kai (1992—), male, master degree candidate, mainly focuses on pulsed laser melting. Email: ue2015work@foxmail.com
Supervisor (Contact author): LI Xiao-hong (1977—), female, professor, Ph.D. degree, mainly focuses on femtosecond laser processing. Email: lixiaohong@swust.edu.cn
Received: Apr.2, 2018; **Accepted**: Jun.8, 2018

donor impurity energy level of the E_c-0.26 eV. The Hall effect measurement shows that the thin film layer has high carrier concentration, over 8×10^{18} cm^{-3}. The Hall effect measurement shows that the thin film layer has high carrier concentration, over 8×10^{18} cm^{-3}.

Key words: Laser physics; Pulsed lasers; Vacuum magnetron; Silicon; Hyper doping; Deep level impurity

OCIS Codes: 160.6990; 260.3060; 310.6860; 350.6050; 140.3460; 140.3390

0 Introduction

At present, the highest efficiency of silicon-basedsolar cells is only 26.3%[1]. One of the reasons for limiting of photoelectric efficiency is that the band gap of silicon is 1.12 eV which makes silicon can not absorb infrared light of wavelength greater than 1 100 nm. For the same reason, the silicon-based photoelectric sensor can not respond to the infrared light with wavelength greater than 1 100 nm[2]. In 1997, Luque A proposed an effective way to improve the infrared absorption by intermediate band, which makes the process of absorbing photons with energy below the band gap possible[3-4]. The theoretical photoelectric efficiency of Intermediate Band Solar Cell (IBSC) can exceed 60%[5]. Impurity intermediate band is an effective way to prepare materials of intermediate band by hyper-doping of deep energy level impurity in silicon[6]. The impurity intermediate band could form a "ladder" in forbidden band to enhance the infrared absorption of silicon[4].

In recent years, there are many studies on the doping of deep level impurities in silicon, in which titanium and sulfur are often used in hyper-doping in silicon[7-9]. In 2017, ZHANG Ting reported that sulfur doping in silicon by femtosecond laser to enhance the infrared response in large wavelength range has been realized[10]. But SULLIVAN J T pointed out that the energy levels of sulfur in silicon are shallow and those of titanium in silicon are closer to the intermediate of the band gap. Therefore, titanium is a better choice for the intermediate band of silicon than sulfur[11]. The required concentration of hyper-doping is about 5×10^{19} cm^{-3} exceeding the solid solubility of deep energy level impurity in silicon which is merely about 10^{16} cm^{-3}[12]. For elements with such low solubility, it is not easy to achieve the high doping concentration required for impurity intermediate band by thermal equilibrium technology. At present, there are some kinds of non-equilibrium technology which could be used in hyper-doping of deep energy level impurity such as ultrashort pulsed laser hyper doping, ion implanting followed by pulsed laser melting, and pulsed laser mixing[13-15]. For example, in 2017, YU Xin-yue used the femtosecond laser to prepared gold hyper-doped black silicon material with high infrared absorption, but the thickness of the doped layer is less than 100 nm[16]. Currently, the combination of ion implantation and ultraviolet pulse laser melting is one of the most common methods for deep level impurity doping. For instance, in 2014, UMEZU I used the ion implantation and 355 nm pulse laser melting to dope titanium in silicon. However, due to the limited penetration depth of ion implantation and ultraviolet wavelength laser, the thickness of the doped layer is very low, less than 200 nm generally. Too thin doping layer should have very limited absorption of light. And the distribution of titanium atoms is uneven, the impurity with doping concentrations below the Mott limit will act as composite center, reducing the electrical properties of materials. Therefore, the homogeneous distribution of doping impurities is very important[17].

In this paper, a new hyper-doping method of magnetron sputtering combined with the 532 nm nanosecond Pulsed Laser Melting (PLM) is developed. The magnetron sputtering is easy to control the thickness of the film and the proportion of silicon and titanium. Moreover, it allows the titanium atom to diffuse fully in the film because of the loose and porous properties of amorphous silicon film. The light absorption coefficient of 532 nm laser in silicon is smaller than that of ultraviolet laser, and the penetration depth for 532 nm laser is larger than that for ultraviolet laser, about 500 nm[18]. The titanium atom concentration in the prepared titanium doped silicon material is above 5×10^{20} cm^{-3}. The thickness of doping layer is over 200 nm, which is higher than previous research. The concentration of titanium varies less than 20% and the distribution of titanium atom is homogeneous. In the wavelength greater than 1 100 nm, the highest absorption coefficient is close to 1.2×10^{4} cm^{-1}, so it increases effectively the infrared absorption performance of silicon materials.

1 Experiments

The sandwich structure of this thin film is shown in fig. 1. Double-sided polishing n-type monocrystalline silicon (111) slice with a thickness of 400 μm ($\rho=5\sim10$ Ω·cm, $n=5\times10^{15}$ cm^{-3} at room temperature) is used as the substrate for magnetron sputtering (JGP-560B, Sky Technology Development, China). Three layers (amorphous silicon, titanium, amorphous silicon) were deposited alternately on the Si substrate. The thickness of amorphous silicon film is 250 nm and that of titanium film is 2.5 nm. The atom content of titanium of thin film is about 0.5%. These three layers Si-Ti-Si form a sandwich structure. The sputtering power of silicon is 100 W and that of titanium is 60 W, the flow rate of argon of silicon and titanium is 40 sccm, and the sputtering time of silicon is 11 min and that of titanium is 30 s. The purity of silicon and titanium target material is higher than 99.995%. After sputtering, these samples are melted by Nd:YAG nanosecond pulsed laser (Quanta-Ray Pro Series, Spectra Physics, USA, wavelength of 532 nm, frequency of 10 Hz, and laser pulse width of 20 ns). The parameters of pulsed laser include five kinds of energy density (0.2 J/cm^2, 0.25 J/cm^2, 0.3 J/cm^2, 0.35 J/cm^2, 0.4 J/cm^2) and two kinds of laser scanning speed (0.05 mm/s, 0.01 mm/s). And the size of the laser facula is 1 mm×10 mm. In addition, the sample was annealed (500℃, 10 min) before PLM. The experimental parameters of all samples are listed in Table 1. Infrared light absorption characteristics of samples has been analyzed by UV-3150 infrared spectrophotometer in wavelength range of 1000～2000 nm (Shimadzu Corporation, Japan). The structural properties of film samples were measured by Glancing Incidence X-ray Diffraction (GIXRD) (X Pert Pro, PANalytical B.V, Netherlands) at the angle of glancing incidence (ω) of 1°. The carrier concentration was measured by HMS-3000 Hall Effect Measurement System (ECOPIA, Korea). The atom concentration of titanium of sample were measured by X-ray Photoelectron Spectroscopy (XPS) (ESCALAB 250Xi, Thermo Fisher Scientific, USA). The thickness of film samples is measured by Scanning Electron Microscope (SEM) (UItra55, Carl zeiss, Germany).

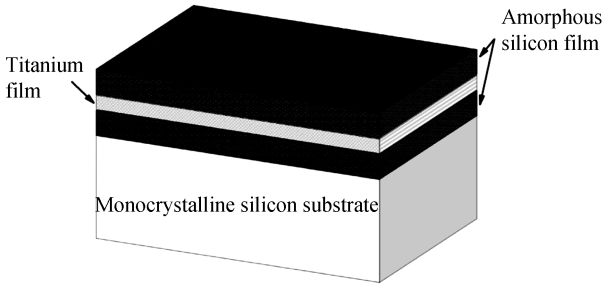

Fig.1 The sketch of the structure of Si-Ti-Si

Table 1 The fabrication parameters of samples

Sample	No.1	No.2	No.3	No.4	No.5	No.6	No.7
Energy density (J/cm^2)	0.2	0.25	0.3	0.3	0.3	0.35	0.4
Scanning speed (mm/s)	0.05	0.05	0.05	0.05	0.01	0.05	0.05
Thermal annealing	-	-	-	500℃,10 min	-	-	-

2 Results and discussion

2.1 Structural properties

Fig. 2 shows that the GIXRD diffraction pattern for all film samples. All the film samples have a very visible crystallization peaks at 56.1°. Calculated by software of JADE6.0, the diffraction peak at 56.1° corresponds to the crystal face (311) of silicon. In addition, there are some small diffraction peaks in other locations of the diffraction pattern, but the intensities of them are too much weaker than that of the peak at 56.1°. The crystal face and chemical composition of all diffraction peaks of samples are shown in Fig. 2. It is easy to see that the thin film of sample has no

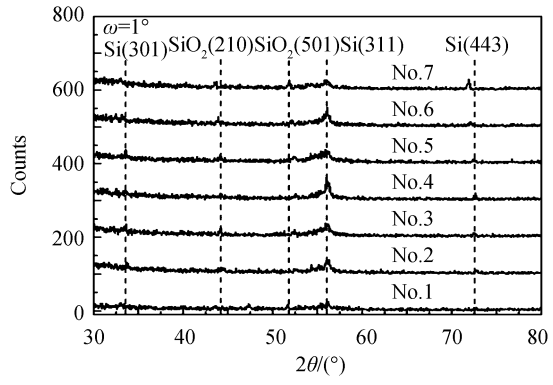

Fig.2 The GIXRD diffraction pattern for all samples with the angle of glancing incidence $\omega=1°$

compound of titanium. The positions of diffraction peak of some samples offset relative to other samples, which should be due to silicon lattice distortion caused by impurity doping. Overall, the thin film layer of samples has crystallized partially.

The crystallinity of all film samples are fitted by using JADE6.0, and these datas are shown in Table 2. The crystallinity of the samples (No.3-No.5) with laser energy density of 0.3 J/cm^2 are all higher than that of other samples with lower or higher energy density. The samples No.1 and No.7 have the lowest crystallinity, they are 4.76% and 5.95% respectively. It makes a conclusion that the crystallinity of the thin film increases firstly and then decreases with the increase of laser energy density. Low energy density can not melt the thin film of sample fully. Overhigh energy density will break the lattice structure and the crystallinity will be lower. In the same laser energy of 0.3 J/cm^2, the sample No.5 with low laser scanning speed has the highest crystallinity, about 24.41%. And in the same laser scanning speed of 0.05 mm/s, the crystallinity of the sample No.3 without thermal annealing is very close to that of the sample No.4 with thermal annealing. So, the thermal annealing has no obvious influence on the crystallinity, and the low scanning speed of 0.01 mm/s will promote the crystallinity. Overall, after PLM, crystallization happens in amorphous silicon films, and it shows polycrystalline structure.

Table 2 The crystallinity of all samples

Sample	No.1	No.2	No.3	No.4	No.5	No.6	No.7
Crystallinity %	4.78	9.29	13.07	12.45	24.41	8.26	5.95

Figure 3 shows the Scanning Electron Microscope (SEM) image of sample No.5 (0.3 J/cm^2) and No.7 (0.4 J/cm^2) with different laser energy density. It is clear that the thin film of sample will be peeled partially after PLM. The thickness of film of sample No.5 decreased from 500 nm to 300 nm around with laser energy density of 0.3 J/cm^2. When the laser energy density is 0.4 J/cm^2, the film of sample (No.7) is broken almost entirely. So the crystallinity of thin film of sample will be lower when the laser energy is too high.

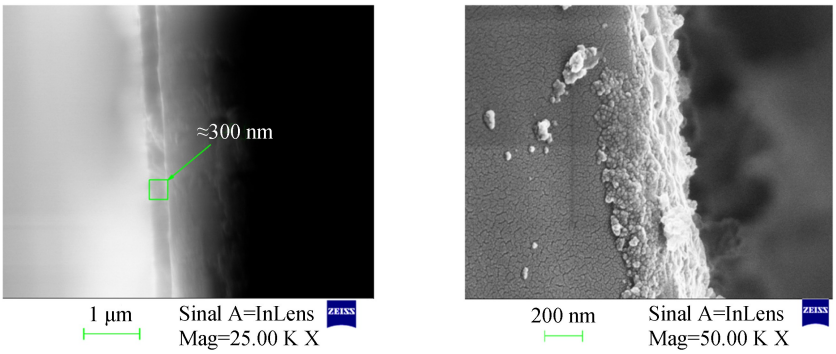

(a) The sample No.5 (b) The sample No.7

Fig.3 The SEM image of samples

Figure 4 shows the depth profiling pattern of the sample (No.5) after PLM measured by X-ray Photoelectron Spectroscopy (XPS), the atom concentration and the atom percentage of titanium of sample are shown in Figure 4. Combined with the result of GIXRD, the thin film of sample has no compound of titanium. After PLM, the atom percentage of titanium of sample is more than 1% in the range of depth of 220 nm around, so that the atom concentration of titanium doping in silicon is more than 5×10^{20} cm^{-3}. This concentration of titanium atom is higher than the hyper-doping concentration of titanium in silicon. And the

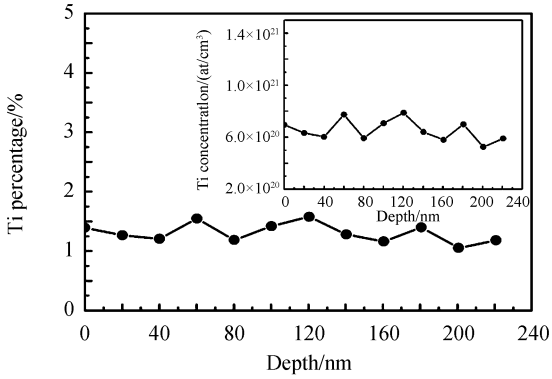

Fig.4 The atom concentration and the atom percentage of titanium of sample after PLM

thickness of hyper-doping layer is more than 200 nm. Furthermore, the distribution of titanium atom is very homogeneous. The varies range of concentration is less than 20% around. Obviously, the method of magnetron sputtering combined with pulsed laser melting can effectively achieve the hyper-doping of titanium in silicon with high thickness of hyper-doping layer and homogeneous distribution of titanium atom.

2.2 Infrared absorption properties

Fig. 5 shows the infrared reflectivity of all samples and the monocrystalline silicon wafer without coating in the wavelength range of 1 000～2 000 nm. The reflectivity of all samples are lower than that of monocrystalline silicon wafer. When the laser energy density increases, the reflectivity of the samples decreases firstly and then increases until it is close to that of silicon wafer. The reflectivity of samples (No. 3～No.5) with laser energy density of 0.3 J/cm^2 is less than that of the other samples with lower or higher energy density. In the same energy density (0.3 J/cm^2), the thermal annealing makes the reflectivity of No.4 higher than others (No.3 and No.5), and when the laser scanning speed (0.01 mm/s) is low, the reflectivity of the sample No.5 is also the lowest in all samples. Figure 6 shows the infrared transmittivity in the same wavelength range. The situation is similar. The transmittivity of samples is lower than that of silicon wafer. The transmittivity of the samples (No.3～No.5) with the energy density of 0.3 J/cm^2 is the lowest, and the sample No.5 with low scanning speed (0.01 mm/s) has the lowest transmittivity. So, the reflectivity and transmittivity of all samples are lower than monocrystalline silicon.

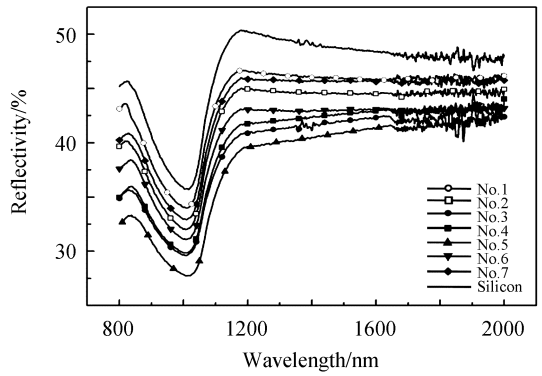

Fig.5 The spectra of the reflectivity

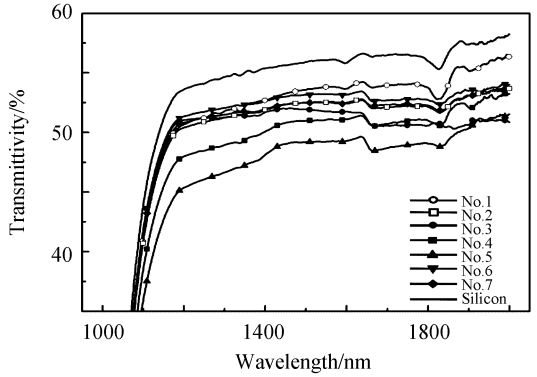

Fig.6 The spectra of the transmittivity

In Fig. 7, subtracting the light absorption coefficient (α) of silicon from that of samples obtains the light absorption coefficient of titanium-doped silicon thin film. The infrared absorptivity of all the samples is higher than that of silicon wafer and the sample without PLM. It can be seen more clearly that, in the wavelength larger than 1 200 nm, the infrared absorption coefficient of the thin film layer is more than 3×10^3 cm^{-1}. The maximum of the light absorption coefficient is close to 1.2×10^4 cm^{-1}. When the energy density is 0.3 J/cm^2, the light absorption coefficient of the samples (No.3～No.5) is higher than others. The higher or lower laser energy leads to lower light absorption coefficient. In a word, the infrared absorption coefficient of the thin film layer of samples increases firstly and then decreases when the laser energy density increases from 0.2 to 0.4 J/cm^2, and the absorption coefficient reach the highest when the energy is 0.3 J/cm^2.

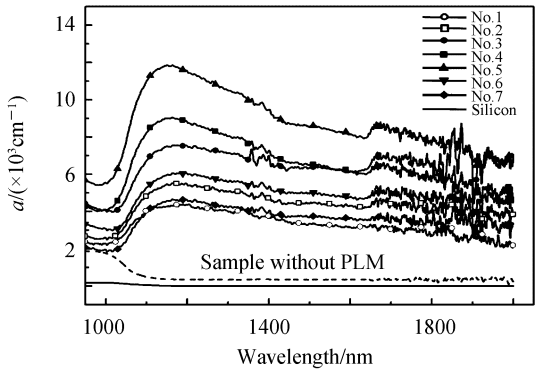

Fig.7 The light absorption coefficient of the thin film wafer of samples and silicon

In the same laser energy of 0.3 J/cm^2, the sample No.5 with low laser scanning speed of 0.01 mm/s has the highest light absorption coefficient of 1.16×10^4 cm^{-1}. In the laser scanning speed of 0.05 mm/s, the absorption of the sample No.4 with thermal annealing is close to that of the sample No.3 without

thermal annealing, and the light absorption coefficient curves of No.3 and No.4 have an intersection in the wavelength of 1 560 nm around. Such relations show that the light absorption coefficient is higher when the laser scanning speed is 0.01 mm/s. Moreover, the light absorption coefficient curves of samples (No.1～No.3, No.6～No.7) are more horizontal than those samples of No.4 and No.5. The absorption coefficient curves of samples No.4 and No.5 have a downward trend when the wavelength is increasing.

The absorption curves of samples No. 4 and No. 5 show clearly that the additional absorption enhancements originate from the sub-band. Moreover, there exists donor impurity energy band of E_c-0.27 eV to E_c-0.26 eV of titanium in silicon[11]. So, the energy gap width of the sub-band of samples has been calculated to verify the existence of the impurity energy levels. The method of Tauc Plot is used to calculate the energy gap width of sub-band (E_g)[19]. The formula of Tauc Plot is given, where α is light absorption coefficient of sample, h is the plank's constant, and v is the frequency of infrared light. Figure 8 gives the plot of hv and $(\alpha hv)^{1/2}$ of the sample No.5.

$$(\alpha h\nu)^{\frac{1}{2}} = A(h\nu - E_g) \tag{1}$$

Extrapolating the straight line of absorption edge of the graph to the abscissa axis to obtain that the energy gap width of sub-band of sample is 0.89 eV around. This value is very close to the donor impurity energy level of the E_c-0.26 eV generated from titanium doped in silicon. This energy level serves as a "ladder" to enhance the absorption of silicon for the lower energy infrared photons. So, the infrared absorption coefficient of silicon materials becomes higher. Overall, the results show that the doping energy level exists in the samples, and enhances the infrared absorption of silicon thin film layer.

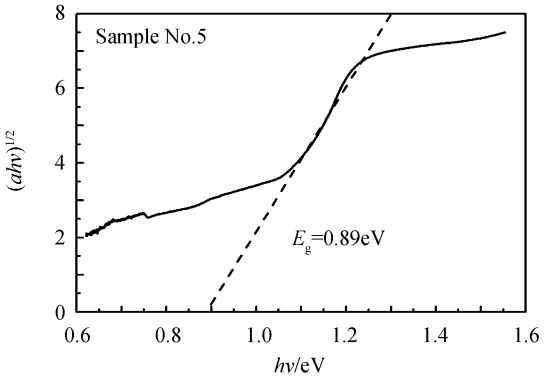

Fig.8 The graph of Tauc Plot method of the sample

2.3 Hall effect properties

Table 3 shows Hall effect data. The carrier concentration of all film samples outclasses that of monocrystalline silicon, and the sheet resistance lower than that of silicon. Titanium is usually to play as a donor impurity in silicon, and therefore the main carrier is electron and the carrier concentration is negative[20-21]. When the laser energy density increases, the carrier concentration will decrease. For samples (No.3～No.5) with laser energy density of 0.3 J/cm^2, the carrier concentration is close and higher than that of other samples with lower or higher laser energy density. Combined with Figure 7, the sample No.5 has the highest carrier concentration and infrared absorption in all samples. Obviously, it's easy to see that when the infrared absorption coefficient of the samples increases, the carrier concentration will show an increasing trend. For the samples (No.3～No.5), the carrier concentration is more than 5×10^{18} cm^{-3}. So, the concentration of titanium in the samples (No.3～No.5) is very high.

Table 3 The electrical datas of samples and the substrate silicon, including carrier concentration, mobility, and sheet resistance

Sample	Carrier concentration/cm^{-3}	Mobility/(cm^2 · V^{-1} · s^{-1})	Sheet resistance/(Ω · □$^{-1}$)
No.1	-2.82×10^{18}	1.21×10^3	91.15
No.2	-1.55×10^{18}	1.31×10^3	76.7
No.3	-7.12×10^{18}	8.59×10^2	59.98
No.4	-6.26×10^{18}	8.56×10^2	58.23
No.5	-8.43×10^{18}	7.18×10^2	51.6
No.6	-3.84×10^{18}	1.36×10^3	59.19
No.7	-2.81×10^{18}	1.33×10^3	82.15
Silicon	-5×10^{15}	4.56×10^3	105.4

3 Conclusions

In this paper, a new kind of hyper-doping technology is proposed to prepare titanium hyper-doped silicon films by combining magnetron sputtering and pulsed laser melting. The results show that the crystallinity of silicon films is about 25% after pulse laser treatment. The titanium concentration of sample is more than 1% (about 5×10^{20} cm^{-3}), higher than the hyper-doping concentration of titanium in silicon. The thickness of hyper-doping layer is more than 200 nm, which improves significantly than previous studies. The distribution of titanium atom is very homogeneous and the concentration change is less than 20%. This means that this novel hyper-doping process can not only achieve higher thickness of doping layer, but also control the uniformity of the impurities atoms doped in silicon. And it can obtain the hyper-doped silicon materials with excellent structural properties, which has great significance for the research of the impurity intermediate band materials. Furthermore, the infrared absorption of thin film samples isenhanced obviously in wavelength larger than 1 100 nm. The highest light absorption coefficient is about 1.16×10^{4} cm^{-1}. The samples show a sub-band with the energy gap width of 0.89 eV. Obviously, the good performance of doping layer can promote the infrared absorption effectively, and it forms the impurity intermediate band in silicon material. The titanium-doped silicon films with good photoelectric properties are hopefully used in photoelectric devices.

References

[1] GREEN M A, EMERY K, HISHIKAWA Y, *et al*. Solar cell efficiency tables (version 49)[J]. *Progress in Photovoltaics Research & Applications*, 2017, **25**(7):905-913.

[2] CSUTAK S M, SCHAUB J D, WU W E, *et al*. High-speed monolithically integrated silicon photoreceivers fabricated in 130-nm CMOS technology[J]. *Journal of Lightwave Technology*, 2002, **20**(9):1724-1729.

[3] GREEN M A. Third generation photovoltaics: advanced solar energy conversion[J]. *Physics Today*, 2006, **57**(12):71-72.

[4] LUQUE A, MARTI A, STANLEY C. Understanding intermediate-band solar cells[J]. *Nature Photonics*, 2012, **6**(3):146-152.

[5] LUQUE A, MARTI A. Increasing the efficiency of ideal solar cells by photon induced transitions at intermediate levels [J]. *Physical Review Letters*, 1997, **78**(26):5014-5017.

[6] WANG Ke-fan, SHAO He-zhu, LIU Kong, *et al*. Possible atomic structures responsible for the sub-bandgap absorption of chalcogen-hyperdoped silicon[J]. *Applied Physics Letters*, 2015, **107**(11):9901-347.

[7] GARCIAHEMME E, GARCIAHERNANSANZ R, OLEA J, *et al*. Room-temperature operation of a titanium supersaturated silicon-based infrared photodetector[J]. *Applied Physics Letters*, 2014, **104**(21):211105-211105-5.

[8] LI Si-yu, WU Zhi-ming, DU Ling-yan, *et al*. Research on photoelectric characteristics of (S, Se) co-doped silicon fabricated by femtosecond-laser irradiation[J]. *Journal of Materials Science Materials in Electronics*, 2018(1):1-6.

[9] SHEEHY M A, TULL B R, FRIEND C M, *et al*. Chalcogen doping of silicon via intense femtosecond-laser irradiation [J]. *Materials Science & Engineering B*, 2007, **137**(1):289-294.

[10] ZHANG Ting, WASEEM A, LIU Bo-han, *et al*. Broadband infrared response of sulfur hyperdoped silicon under femtosecond laser irradiation[J]. *Materials Letters*, 2017, **196**:16-19.

[11] SULLIVAN J T, SIMMONS C B, BUONASSISI T, *et al*. Targeted search for effective intermediate band solar cell materials[J]. *IEEE Journal of Photovoltaics*, 2014, **5**(1):212-218.

[12] SHER M J, MAZUR E. Intermediate band conduction in femtosecond-laser hyperdoped silicon[J]. *Applied Physics Letters*, 2014, **105**(3):1850-130.

[13] LIMAYE M V, CHEN S C, LEE C Y, *et al*. Understanding of sub-band gap absorption of femtosecond-laser sulfur hyperdoped silicon using synchrotron-based techniques.[J]. *Scientific Reports*, 2015, **5**:11466.

[14] LI Xiao-hong, CHANG Li-yang, QIU Rong, *et al*. Microstructuring and doping of silicon with nanosecond laser pulses [J]. *Applied Surface Science*, 2012, **258**(20):8002-8007.

[15] HU Shao-xu, HAN Pei-de, GAO Li-peng, *et al*. The effects of femtosecond laser irradiation and thermal annealing on the optoelectronic properties of silicon supersaturated with sulfur[J]. *Chinese Physics Letters*, 2012, **29**(4):046101-379.

[16] YU Xin-yue, ZHAO Ji-hong, LI Chun-hao, *et al*. Gold-hyperdoped black silicon with high IR absorption by femtosecond laser irradiation[J]. *IEEE Transactions on Nanotechnology*, 2017, **16**(3):502-506.

[17] UMEZU I, NAITO M, KAWABE D, *et al*. Hyperdoping of silicon with deep-level impurities by pulsed YAG laser melting[J]. *Applied Physics A*, 2014, **117**(1):155-159.

[18] BUCHER K, BRUNS J, WAGEMANN H G. Absorption coefficient of silicon: An assessment of measurements and

the simulation of temperature variation[J]. *Journal of Applied Physics*, 1994, **75**(2):1127-1132.

[19] TAUC J, GRIGOROVICI R, VANCU A. Optical properties and electronic structure of amorphous germanium[J]. *Physica Status Solidi*, 1966, **15**(2):627 - 637.

[20] CHEN J W, MILNES A G, ROHATGI A. Titanium in silicon as a deep level impurity[J]. *Solid-State Electronics*, 1979, **22**(9):801-808.

[21] OKUYAMA M, MATSUNAGA N, CHEN J W, *et al*. Photoionization cross-sections and energy levels of gold, iron, platinum, silver, and titanium in silicon[J]. *Journal of Electronic Materials*, 1979, **8**(4):501-515.

引用格式:WANG Kai, LI Xiao-hong, ZHANG Yan-bing, *et al*. Study of Titanium-doped Silicon Films Prepared by Magnetron Sputtering and Nanosecond Pulsed Laser[J]. *Acta Photonica Sinica*, 2018, **47**(9):0916005

王凯,李晓红,张延彬,等.磁控溅射结合脉冲激光制备钛掺杂硅薄膜的研究[J].光子学报,2018,**47**(9):0916005